

Mach Disk in Truncated Plug Nozzle Flows

Thomas V. Giel Jr.* and Thomas J. Mueller†
University of Notre Dame, Notre Dame, Ind.

The first shock reflection within truncated plug nozzle propulsive jets is investigated experimentally using a free jet blowdown facility. The locations and sizes of these reflections in axisymmetric plug nozzles, with cylindrical shrouds and conical truncated plugs, are presented. Data are presented for a range of ambient to nozzle total pressure ratios. The effects on Mach disk location and size resulting from changing plug length and from varying amounts of base bleed are documented.

Nomenclature

A	= area
L	= plug length from the geometric throat
L_{\max}	= length of the untruncated conical plug
M	= Mach number
P	= pressure
r	= radius
X	= axial coordinate along the nozzle axis with origin at the shroud exit plane

Subscripts

at	= atmospheric conditions
b	= conditions at the base of the plug
md	= refers to Mach disk
ne	= nozzle shroud exit conditions
nt	= nozzle throat conditions
01	= test nozzle stagnation conditions
sh	= nozzle shroud

Introduction

EFFICIENT exhaust nozzle performance over a wide range of ambient operating conditions is a major requirement for advanced propulsion systems. Analyses and tests¹⁻⁴ have demonstrated that altitude compensating nozzles can fulfill this requirement. One altitude compensating nozzle is the truncated plug (T-P) or aerospike nozzle, which appears particularly attractive because it is short, lightweight, and relatively easy to cool. Furthermore, T-P nozzles can be designed as the entire vehicle base in either axisymmetric or nonaxisymmetric configurations, thus alleviating the flow interference and base heating problems of clustered nozzles.⁵

However, improved understanding of the T-P nozzle flowfield is necessary in order to optimize design. This understanding is lacking because plug nozzle flowfields are highly nonuniform, contain a viscous separated flow region (near wake), and contain multiple shocks. In addition, the nozzle can operate in both the "open" and "closed" wake configurations.³⁻⁵ At high values of ambient pressure ratio, P_{at}/P_{01} , the separated wake region is in the "open" con-

figuration (i.e., sensitive to ambient conditions). As the ambient pressure ratio decreases, the shear layer between the exhaust flow and the wake converges on the nozzle axis and eventually "closes" the wake to ambient influen. Once the wake is "closed", the plug base pressure remains relatively constant as the ambient pressure ratio decreases. For most T-P nozzle applications, the wake would be "closed" for the major portion of the flight. The near wake is more clearly defined in the "closed" than in the "open" configuration, but even this configuration is difficult to treat analytically.^{3,6} Therefore, experimental data are necessary both to improve understanding of the flow and to evaluate analytical models.

One conspicuous structure in "closed" wake T-P nozzle flowfields is the first Mch disk.⁷ A qualitative analysis of the shadowgraphs obtained by Mueller, et al.⁴ indicates that the Mach disk structure characterizes the T-P nozzle "closed" wake exhaust flowfield. For example, as the ambient pressure ratio, P_{at}/P_{01} , decreases, the Mach disk moves downstream and grows in diameter while the jet external boundary plumes away from the nozzle centerline. Occurrence of a regular reflection indicates that the nozzles studied are operating reasonably close to the "open" wake configuration,^{4,7} and a small ambient pressure ratio increase will "open" the wake.

The phenomenon of the Mach disk appears when the internal shock wave generated near the corner of an axisymmetric nozzle shroud is too strong to be regularly reflected at the centerline. For T-P nozzles, as for converging-diverging (C-D) bell nozzles, left running expansion waves reflect from the freejet boundary as compression waves which coalesce to generate the internal shock. Thus the Mach disk structure for T-P nozzles can be expected to have similarities to the C-D nozzle disk behavior, (well documented in both un-

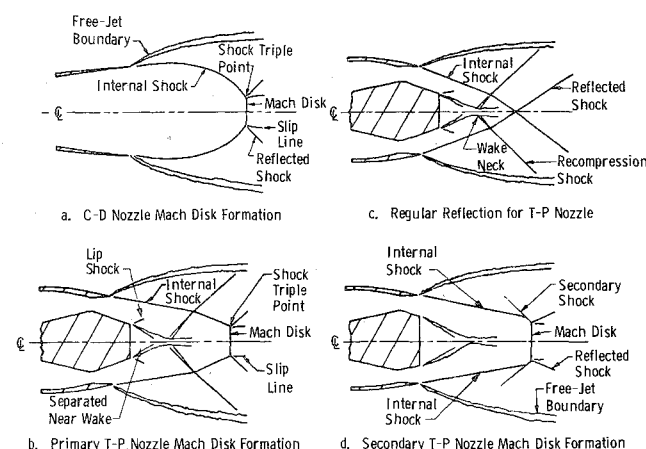


Fig. 1 Shove interactions for axisymmetric C-D and T-P nozzles.

Presented as Paper 75-886 at the AIAA 8th Fluid and Plasma Dynamics Conference, Hartford, Conn., June 16-18, 1975; submitted June 26, 1975; revision received November 6, 1975. This research was jointly supported by NASA under contract NAS8-25601 and the Department of Aerospace and Mechanical Engineering, and was part of the M.S. thesis of the first author.

Index Categories: Advanced Space Propulsion; Supersonic Air-breathing Propulsion; Jets, Wakes, and Viscid-Inviscid Interactions.

*NDEA Fellow. Presently Research Engineer, Engine Test Facility, ARO, Inc., Arnold Engineering Development Center, Arnold Air Force Station, Tenn. Member AIAA.

†Professor, Department of Aerospace and Mechanical Engineering. Associate Fellow AIAA.

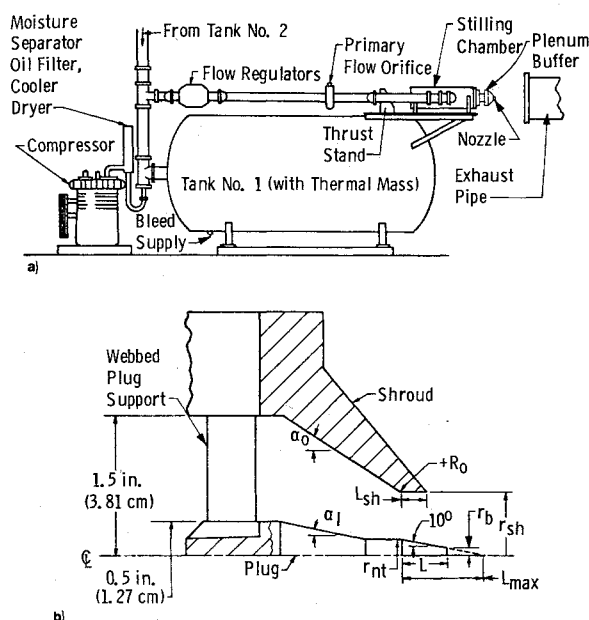


Fig. 2 Test apparatus: a) sketch of nozzle thrust facility; b) schematic of test nozzles.

Table 1 Axisymmetric truncated plug nozzle model ATP 1

Overall area ratio, $A_{sh}/A_{nt} = 1.555$ ($A_{sh} = \pi r_{sh}^2$)
Design Mach number, $M_d = 1.9$
Shroud expansion ratio, $P_{ne}/P_{01} = 0.251$
Throat area, $A_{nt} = 0.33$ in. ² (2.13 cm ²)
Shroud radius, $r_{sh} = 0.405$ in. (1.03 cm)
Plug throat radius, $r_{nt} = 0.242$ in. (0.615 cm)
Shroud length from throat, $L_{sh} = 0.30$ in. (0.76 cm), $L_{sh}/r_{sh} = 0.74$
Maximum plug length, $L_{max} = 1.374$ in. (3.49 cm)
$R_0 = 0.31$ in. (0.79 cm)
$\alpha_0 = 33.25^\circ$
$\alpha_1 = 12.3^\circ$

Length ratio, L/L_{max}	Plug dimensions, in. (cm) Length from throat, L , in. (cm)	Base radius, r_b , in. (cm)
0.22	0.300 (0.76)	0.188 (0.48)
0.28	0.380 (0.96)	0.174 (0.44)
0.33	0.450 (1.14)	0.162 (0.41)
0.38	0.520 (1.32)	0.150 (0.38)
0.43	0.590 (1.50)	0.137 (0.35)
0.48	0.660 (1.68)	0.125 (0.32)

^a M_d based on total exit area/nozzle throat area ratio (A_{sh}/A_{nt}).

^b P_{ne}/P_{01} based on shroud exit area/nozzle throat area ratio.

Table 2 Axisymmetric truncated plug nozzle model ATP 2

Overall area ratio, $A_{sh}/A_{nt} = 1.684$ ($A_{sh} = \pi r_{sh}^2$)
Design Mach number, $M_d = 2$
Shroud expansion ratio, $P_{ne}/P_{01} = 0.267$
Throat area, $A_{nt} = 0.60$ in. ² (3.88 cm ²)
Shroud radius, $r_{sh} = 0.568$ in. (1.44 cm)
Plug throat radius $r_{sh} = 0.568$ in. (1.44 cm)
Plug throat radius $r_{nt} = 0.36$ in. (0.919 cm)
Shroud length from throat, $L_{sh} = 0.30$ in. (0.76 cm), $L_{sh}/r_{sh} = 0.53$
Maximum plug length, $L_{max} = 2.070$ in. (5.26 cm)
$R_0 = 0.20$ in. (0.51 cm)
$\alpha_0 = 30^\circ$
$\alpha_1 = 6^\circ$

Length ratio, L/L_{max}	Plug dimensions, in. (cm) Length from throat, L , in. (cm)	Base radius, r_b , in. (cm)
0.14	0.300 (0.76)	0.312 (0.79)
0.23	0.482 (1.22)	0.280 (0.71)
0.28	0.573 (1.45)	0.260 (0.66)
0.33	0.678 (1.72)	0.245 (0.62)
0.38	0.783 (1.99)	0.227 (0.58)

derexpanded^{8,9} and overexpanded¹⁰ flows). However, the highly nonuniform flow associated with the altitude compensating ability of T-P nozzles³⁻⁵ can be expected to create variations in the disk characteristics peculiar to T-P nozzles. The separate region or wake in the center of the nozzle flowfield (Fig. 1) can interfere with the Mach disk formation, while the existence of several shocks, in addition to the internal shock originating near the shroud corner, can alter the Mach disk orientation. Figure 1 illustrates some of the shock reflections for C-D and T-P nozzles.

The objective of this research was to document the changes in location and size of the Mach disk in jets from plug nozzles with truncated conical plugs and cylindrical shrouds for a range of pressure ratios, P_{at}/P_{01} . Both plug length and shroud exit area ratio were changed. Other investigations^{2,3} have shown that bleeding small amounts of mass into the wake region of T-P nozzles enhances their performance, so the effects of small amounts of base bleed on the Mach disk formation were studied.

Experimental Apparatus

The experiments were performed using the Notre Dame Nozzle Thrust Facility (Fig. 2a). This free jet facility is a blowdown type apparatus exhausting to the atmosphere and capable of providing total pressure up to 11 atm for approximately 30 sec for the larger nozzle used. The primary air flow is metered with an orifice flow meter and the secondary "bleed" air flow is metered with an ASME long radius venturi operating at critical flow conditions. The facility includes a pin hole source shadowgraph system for visual study of the flow including determination of the locations and sizes of the Mach disk. Because such a "point" source system produces finite width bands, rather than sharp lines to indicate shock waves, an error between 2% and 5% is possible in measuring the Mach disk sizes and locations.^{7,11}

Two axisymmetric internal-external expansion plug nozzles, ATP1 and ATP2, were designed for Mach numbers of 1.9 and 2 respectively, based on the overall area ratio, A_{sh}/A_{nt} . The geometry of both nozzles is illustrated in Fig. 2b. Measurements are given in Tables 1 and 2. Six plugs with different length ratios (L/L_{max}) were built for ATP1, and special bleed plugs were constructed to match each of these. The bleed port for each bleed plug covered its entire plug base. Five plugs were built for ATP2, three with length ratios which

matched those of ATP1 plugs. A more complete description of the experimental equipment and procedures may be found in Ref. 7.

Results

The Mach disk phenomenon appears when the jet flow conditions produce an oblique shock which is too strong to be simply reflected from the jet centerline. For both C-D and T-P nozzles the internal shock originating near the shroud exit corner instigates the first Mach disk. The location and size of this first Mach disk is determined by the interaction of the central core and the outer coaxial stream downstream of the disk. Indeed the Mach disk locations and sizes have been predicted in C-D nozzle plumes by requiring this interaction to produce a condition equivalent to choking for the central core flow.^{8,9,12}

The characteristics of the shock reflection occurring in a particular jet flow will be dependent on the nozzle operating characteristics and in particular on ambient pressure ratio P_{at}/P_{01} and nozzle geometry. For T-P nozzles, the Mach disk structure shows pronounced changes with pressure ratio

changes.³⁻⁵ The distance measured along the axis between the shroud exit plane and the Mach disk (X_{md}) decreases as P_{at}/P_{01} increases, as shown in Fig. 3. As expected this trend is the same as that documented for C-D bell nozzles.⁹ Also, as for C-D nozzles, the Mach disk radius decreases as P_{at}/P_{01} increases (Fig. 4). These changes are a consequence of the increase of the radial extent of the jet plume which accompanies a pressure ratio, P_{at}/P_{01} , decrease.

Variations in the shock reflection formation resulting from geometric changes of the T-P nozzles are indicated in Figs. 3, 4, and 5. The variation of the Mach disk location due to L/L_{max} changes is presented in Fig. 3 and qualitatively in Fig. 5. Elongation of the plug just moves the Mach disk farther downstream. This trend is not as obvious in Fig. 3 for ATP2 as for ATP1 because, as Fig. 5c shows, the Mach disk for ATP2 curves into a "bowl" shape for the longer plug lengths, and since the location of the Mach disk, X_{md} , was measured along the nozzle axis, this curvature masked the trend of the downstream movement of the disk with increasing plug length.

Most of the Mach disks for ATP2 exhibited some such "bowl" curvature. This curvature is expected since, for the longer ATP2 plugs, the Mach disk occurs in a highly nonuniform flow region just downstream of the neck of the wake. Flow from the near wake region accelerates through the sonic condition downstream of the neck while the free jet flow is decelerating as it is turned by the recompression shock. For most of the tested ATP1 plugs the Mach disks occurred moderately far downstream from the wave neck, which allowed the flow to achieve fairly uniform conditions upstream of the Mach disk. Thus ATP1 was not expected to show as much disk curvature as ATP2.

The variation in the radii of the Mach disks resulting from L/L_{max} changes is presented in Figs. 4 and 5. As the plug length increases, the Mach disk radii decrease. The Mach disk "bowl" curvature again slightly masks this trend because the nonuniform flow which creates the curvature is asymmetrical for these imperfect nozzles thus skewing the shock triple points (Fig. 5c) into different vertical planes. (The radii of the disks were defined as half the distance between triple points).

An important variation in the Mach disk structure occurring with the shortest plug lengths is shown in Fig. 4. The Mach disk radii are more nearly constant with ATP1, plug

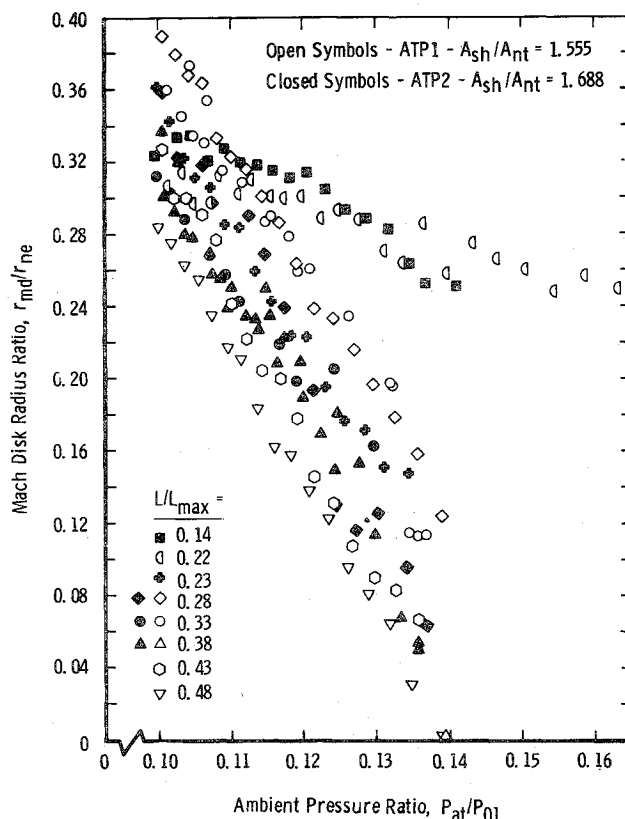


Fig. 4 Effect of ambient pressure ratio on Mach disk radius.

$L/L_{max} = 0.22$, and ATP2, plug $L/L_{max} = 0.14$, throughout the entire pressure ratio (P_{at}/P_{01}) range. Inspection of the shadowgraphs for these two nozzles indicates that the first Mach disk is controlled by the occurrence of a "secondary" shock as illustrated in Fig. 1d. This secondary shock is formed from the same mechanism that generates the internal shock, but it is the expansion waves propagating from the plug lip which produce the secondary shock. These expansion waves can control the disk occurrence only when they are generated far enough upstream to produce a shock which coalesces with the internal shock. This has only been observed to happen for the shortest plugs tested with each nozzle, and both of those plugs were truncated at the shroud exit plane.

Variations in the shock reflection formation were also observed with changes in the nozzle overall area ratio, A_{sh}/A_{nt} . The data in Figs. 3 and 4 indicate that for the same plug length ratios, the Mach disks for ATP2 are closer to the nozzle exit plane and are relatively smaller than those for ATP1. This cannot be entirely credited to the A_{sh}/A_{nt} difference, however, since ATP1 and ATP2 also have different shroud length to nozzle radius ratios and different plug length to nozzle radius ratios. Since those geometric effects cannot be separated from this study, the observed results cannot be interpreted without further investigation.

Influence of Base Bleed

The addition of small amounts of mass (1% of the primary nozzle flow), bled into the near wake region distinctly alters the external nozzle flowfield. The neck of the near wake spreads to accommodate the increased mass flow, decreasing the inclination of the viscous boundary of the wake. The flow angle of the adjacent supersonic flow likewise decreases, apparently (in the case of just 1% bleed) enough to eliminate the need for a strong recompression shock to turn the flow parallel to the nozzle axis. However, the Mach disk structure is formed in the same manner for nozzles with bleed as for nozzles without bleed. Therefore, for the bleed cases, as for

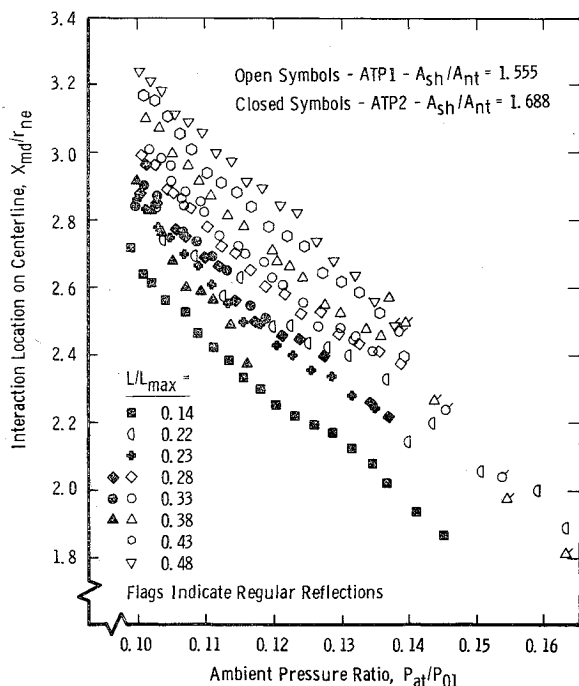


Fig. 3 Effect of ambient pressure ratio on Mach disk location.

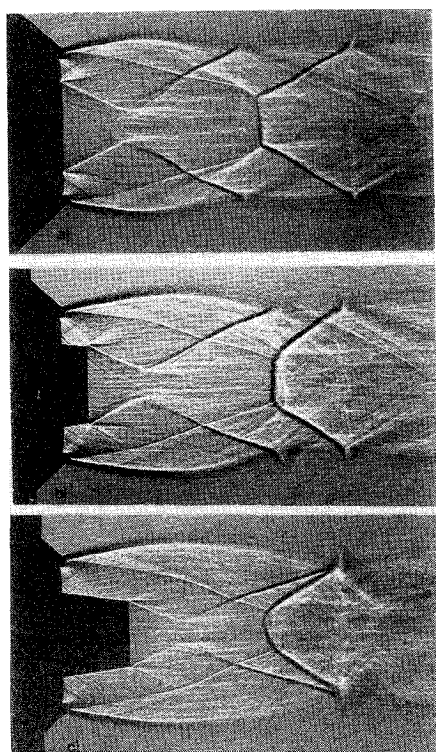


Fig. 5 Shadowgraph sequence of nozzle ATP2 with increasing plus length ($P/P_{01}=0.107$): a) $L/L_{max}=0.14$, no bleed flow; b) $L/L_{max}=0.23$, no bleed flow; c) $L/L_{max}=0.38$, no bleed flow.

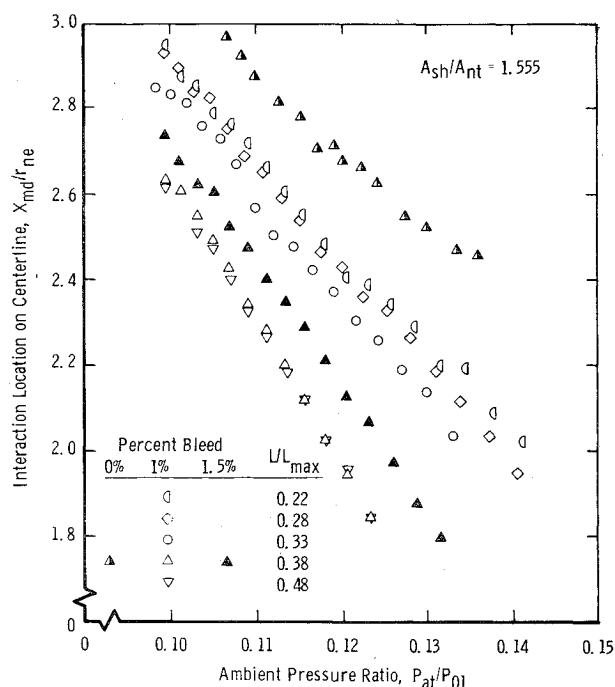


Fig. 6 Effect of ambient pressure ratio on Mach disk location for varying base bleed flow with nozzle ATP1.

the nonbleed cases, the distance to the disk decreases with increasing pressure ratio P_{at}/P_{01} (as shown in Fig. 6), while the disk radius decreases (as shown in Fig. 7). Furthermore, even with bleed, the $L/L_{max}=0.22$ nozzle of ATP1 shows the "secondary" Mach disk formation mode.

Some influences of varying the bleed flow rates (up to 1.5%) were also observed in this study. Changes in the Mach disk locations as a function of base bleed for the $L/L_{max}=0.38$ nozzle are shown in Fig. 6. The $L/L_{max}=0.38$ nozzle was selected to illustrate these trends (which occurred

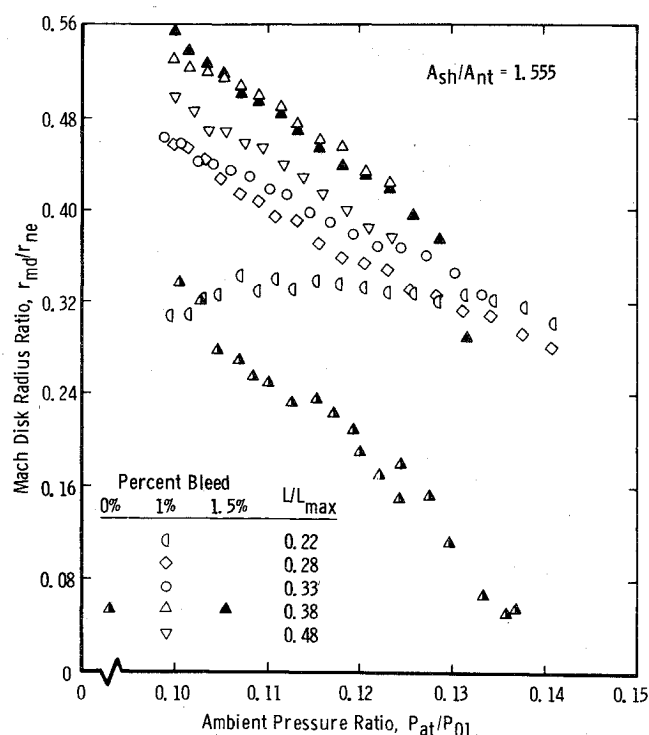


Fig. 7 Effect of ambient pressure ratio on Mach disk size for varying base bleed flow with nozzle ATP1.

with all the geometries). Bleed initially moved the Mach disk upstream from its nonbleed location, but increasing the bleed (from 1% to 1.5%) moved the disk back downstream. This is really only a consequence of the Mach disk curvature, which is more pronounced for 1% bleed than for 1.5% bleed. Initially, with a small amount of bleed, the neck of the near wake moves closer to the Mach disk enhancing the nonuniformity of the flow approaching the Mach disk. But with increased bleed flow the neck of the near wake eventually moves back away from the Mach disk enhancing the uniformity of the flow approaching the disk and diminishing the disk curvature phenomenon. The changes in Mach disk size resulting from changes in the bleed flow rate are documented in Fig. 7 (again for the $L/L_{max}=0.38$ nozzle). Increased bleed flow expands the near wake and thus expands the entire jet flowfield including the distance between the edges or triple points of the Mach disk.

It should be mentioned that the documented changes in the location of the Mach disk with bleed are primarily a result of the definition of X_{md} . If the disk location were to be defined as the axial distance to the shock triple points then the newly defined X_{md} would increase with increasing bleed regardless of the flow alterations which produce disk curvature.

Conclusions

Detailed optical investigations of truncated plug nozzle flowfields provided both qualitative and quantitative data delineating the changes in the first Mach disk structure with changing ambient-to-total-pressure ratio and basic geometric alterations. Both the axial distance separating the nozzle from the disk and the radius of the disk decreased with increasing ambient to total pressure ratio. Elongation of the plug centerbody moved the Mach disk downstream while decreasing the radius of the disk. The longer plugs also enhanced a curving of the disk structure into a "bowl" shape. Two "modes" of formation were discovered for the Mach disk structure and the nozzle geometry determined which "mode" will occur.

Mass bled into the near wake base region tended to enlarge the neck of the wake and diminish the recompression shock. The same basic trends of Mach disk position and size with changing pressure ratio were observed with bleed as were ob-

served without bleed. However, increased bleed altered the disk curvature and increased the disk radius.

References

- ¹Connors, J.F., Cubbison, R.W., and Mitchell, G.A., "Annular Internal-External Expansion Rocket Nozzles for Large Booster Applications," NASA TN D-1049, Sept. 1961.
- ²Wasko, R.A., "Performance of Annular Plug and Expansion Deflection Nozzles Including External Flow Effects at Transonic Mach Numbers," NASA TN D-4463, April 1968.
- ³Hall, C.R. Jr. and Mueller, T.J., "Exploratory Analysis of Nonuniform Plug Nozzle Flowfields," *Journal of Spacecraft and Rockets*, Vol. 9, May 1972, pp. 337-342.
- ⁴Mueller, T.J., Suel, W.P., Fanning, A.E. Giel, T.V., and Galanga, F.L. "Analytical and Experimental Study of Axisymmetric Truncated Plug Nozzle Flow Fields," University of Notre Dame, Notre Dame, Ind. UNDAS TN-029-PR-9, Jan. 1971.
- ⁵Mueller, T.J. and Suel, W.P., "Base Flow Characteristics of a Linear Aerospoke Nozzle Segment," *Transactions of the ASME, Journal of Engineering for Industry*, Series B, Vol. 95, Feb. 1973, pp. 353-359.
- ⁶Sule, W.P. and Mueller, T.J., "Annular Truncated Plug Nozzle Flowfields and Base Pressure Characteristics," *Journal of Spacecraft and Rockets*, Vol. 10, Nov. 1973, pp. 689-695.
- ⁷Giel, T.V., Jr., "Mach Reflections in Axisymmetric Truncated Plug Nozzle Flows," M.S. Thesis, Dept. of Aerospace and Mechanical Engineering, University of Notre Dame, Notre Dame, Ind., May 1973.
- ⁸Abbott, M., "The Mach Disk in Underexpanded Exhaust Plumes," *AIAA Journal*, Vol. 9, March 1971, pp. 512-514.
- ⁹Fox, H., "On the Structure of Jet Plumes," *AIAA Journal*, Vol. 12, Jan. 1974, pp. 105-107.
- ¹⁰Chow, W.L. and Chang, I.S., "Mach Reflections from Overexpanded Nozzle Flows," *AIAA Journal*, Vol. 10, Sept., 1972, pp. 1261-1263.
- ¹¹Weyl, F.J., "Analysis of Shadowgraphs," Sec. A, 1.4, *Physical Measurements in Gas Dynamics and Combustion*, Vol. IX of High Speed Aerodynamics and Jet Propulsion, Princeton University Press, Princeton, N.J., 1954, pp. 20-23.
- ¹²Chow, W.L. and Chang, I.S., "Mach Reflection Associated with Over-Expanded Nozzle Free Jet Flows," *AIAA Journal*, Vol. 13, June 1975, pp. 762-766.

From the AIAA Progress in Astronautics and Aeronautics Series . . .

INSTRUMENTATION FOR AIRBREATHING PROPULSION—v. 34

Edited by Allen Fuhs, Naval Postgraduate School, and Marshall Kingery, Arnold Engineering Development Center

This volume presents thirty-nine studies in advanced instrumentation for turbojet engines, covering measurement and monitoring of internal inlet flow, compressor internal aerodynamics, turbojet, ramjet, and composite combustors, turbines, propulsion controls, and engine condition monitoring. Includes applications of techniques of holography, laser velocimetry, Raman scattering, fluorescence, and ultrasonics, in addition to refinements of existing techniques.

Both inflight and research instrumentation requirements are considered in evaluating what to measure and how to measure it. Critical new parameters for engine controls must be measured with improved instrumentation. Inlet flow monitoring covers transducers, test requirements, dynamic distortion, and advanced instrumentation applications. Compressor studies examine both basic phenomena and dynamic flow, with special monitoring parameters.

Combustor applications review the state-of-the-art, proposing flowfield diagnosis and holography to monitor jets, nozzles, droplets, sprays, and particle combustion. Turbine monitoring, propulsion control sensing and pyrometry, and total engine condition monitoring, with cost factors, conclude the coverage.

547 pp. 6 x 9, illus. \$14.00 Mem. \$20.00 List

TO ORDER WRITE: Publications Dept., AIAA, 1290 Avenue of the Americas, New York, N. Y. 10019